BIOELECTRICITY
Volume 2, Number 1, 2020

DOI: 10.1089/bioe.2019.0024

Original Research

Assessment of Enrichment of Human Mesenchymal Stem Cells Based on Plasma and Mitochondrial Membrane Potentials

Timothy Kamaldinov, BS,[1] Josh Erndt-Marino, PhD,[1–3] Michael Levin, PhD,[3] David L. Kaplan, PhD,[2,3] and Mariah S. Hahn, PhD[1]

Abstract

Background: Human mesenchymal stem cells (hMSCs) are utilized preclinically and clinically as a candidate cell therapy for a wide range of inflammatory and degenerative diseases. Despite promising results in early clinical trials, consistent outcomes with hMSC-based therapies have proven elusive in many of these applications. In this work, we attempt to address this limitation through the design of a stem cell therapy to enrich hMSCs for desired electrical and ionic properties with enhanced stemness and immunomodulatory/regenerative capacity.

Materials and Methods: In this study, we sought to develop initial protocols to achieve electrically enriched hMSCs (EE-hMSCs) with distinct electrical states and assess the potential relationship with respect to hMSC state and function. We sorted hMSCs based on fluorescence intensity of tetramethylrhodamine ethyl ester (TMRE) and investigated phenotypic differences between the sorted populations.

Results: Subpopulations of EE-hMSCs exhibit differential expression of genes associated with senescence, stemness, immunomodulation, and autophagy. EE-hMSCs with low levels of TMRE, indicative of depolarized membrane potential, have reduced mRNA expression of senescence-associated markers, and increased mRNA expression of autophagy and immunomodulatory markers relative to EE-hMSCs with high levels of TMRE (hyperpolarized).

Conclusions: This work suggests that the utilization of EE-hMSCs may provide a novel strategy for cell therapies, enabling live cell enrichment for distinct phenotypes that can be exploited for different therapeutic outcomes.

Keywords: mesenchymal stem cells, mitochondrial membrane potential, plasma membrane potential, enrichment

Introduction

Cell therapy based on mesenchymal stem cells (MSCs) is a promising treatment option for a variety of inflammatory and degenerative disorders. The therapeutic action of MSCs is due, in large part, to their ability to interact with the innate and adaptive arms of the immune system as well as delivery of regenerative cues through mostly paracrine signaling.[1] In addition, their ability to differentiate into different cell types, including osteoblasts, chondrocytes, myoblasts, stromal cells, and neurons, among others, contributes to their utility for clinical applications.[2] Having demonstrated some success in preclinical and early clinical trials,[3–6] human MSCs (hMSCs) suffer from population heterogeneity, and this may contribute to variable clinical outcomes. Clinical trials typically inject about 1 to 5×10^6 MSCs/kg of body weight,[7–12] which must be expanded from about 50,000 MSCs collected from 18 to 55 mL of aspirated bone marrow.[13–15] This indispensable expansion step may last several weeks and it is associated with the onset of cell senescence,[16] spontaneous differentiation,[17] loss of stemness,[18] and the general decrease in capacity of the MSCs to interact favorably with the immune system and target tissues.[19] In addition, MSCs can also be heterogeneous within the same population in terms of multipotency and differentiation potential,[20,21] cell size and proliferation rates,[22,23] metabolism,[24] and immunomodulatory capacity.[25]

[1]Department of Biomedical Engineering, Rensselaer Polytechnic Institute, Troy, New York.
[2]Department of Biomedical Engineering, Tufts University, Medford, Massachusetts.
[3]Allen Discovery Center at Tufts University, Department of Biology, Tufts University, Medford, Massachusetts.

Collectively, the theme(s) that emerge from these and many other studies are that (i) our current knowledge of what factors render hMSCs most effective for therapy is incomplete, and (ii) some subpopulations within MSC colonies can be more therapeutically beneficial than others. Hence, efforts are needed to deepen and integrate knowledge of stem cell state by monitoring factors from different cell processes to identify and enrich specific subpopulations for clinical applications.

The overarching hypothesis of this work is that cell state can be defined, in part, by electrical and ionic biophysical parameters due to their established, emerging, and proposed role(s) in the regulation of a myriad of cell[26–46] and physiological processes.[47–55] In terms of stem cell state, undifferentiated stem cells with greater proliferative capacity (than their differentiated progeny) have been suggested to be associated with a depolarized plasma membrane, while terminally differentiated and quiescent cells tend to be hyperpolarized.[53] This relationship may be true for hMSCs as well; modulation of plasma membrane potential via pharmaceuticals or changing the ionic milieu has been shown to be able to override biochemical signaling to prevent hMSC differentiation,[47] or suppress their differentiated state,[56] even in the presence of the most potent chemical mediators known to drive differentiation down certain lineages. In addition, mitochondrial membrane potential may also be involved in differentiation and immunomodulatory functions of hMSCs. For example, hyperpolarization of mitochondrial membrane potential has been associated with osteogenic differentiation of hMSCs.[57] Finally, the mitochondrial membrane depolarized within a population of hMSCs in response to aggregation,[58,59] a process known to preserve stemness[60,61] and enhance immunomodulatory and regenerative capacity of hMSCs.[58,62,63]

Thus, the specific hypothesis of this study was that hMSCs isolated with depolarized electrical properties will exhibit features of reduced senescence, enhanced stemness, and improved immunomodulatory capacity. Here, we report the development of a strategy for generating electrically enriched hMSCs (EE-hMSCs) based on fluorescence-activated cell sorting (FACS) with tetramethylrhodamine, ethyl ester (TMRE), a lipophilic, cationic, nontoxic, fluorescent indicator of plasma and mitochondrial membrane potentials ($\Delta\Psi$). While few studies have been performed to isolate therapeutically competent MSCs before or during expansion,[64–67] it is unknown if enrichment before injection after adequate cell numbers were achieved can improve therapies. Enrichment at this stage, rather than at the isolation stage, may be more appropriate because of the expansion needed to achieve adequate cell numbers. After determining the feasibility of the sorting procedures, the differences in phenotypes of populations with high and low TMRE intensities were investigated.

Materials and Methods

MSC culture

Cryopreserved human bone marrow-derived MSCs (Texas A&M Institute for Regenerative Medicine) from donors 7071L, 8004L, and 8001R were thawed and expanded in minimum essential medium-α (Gibco) supplemented with 16.5% MSC-qualified fetal bovine serum (FBS Premium Select; Atlanta Biologicals), 1% antibiotic solution (10,000 IU/mL penicillin and 10,000 μg/mL streptomycin; Life Technologies), and 1% glutamine (GlutaMAX; Life Technologies) in a 37°C, 5% CO_2-jacketed incubator.[68] Cells were grown to 70–85% confluence and then harvested with TrypLE Express (Gibco) and replated for further expansion using a 1:4 split. At passages 5–6, MSCs were harvested for FACS. The specific passage numbers for electrical enrichment were chosen according to current cell therapy standards.[69]

FACS of hMSCs

Human bone marrow-derived MSCs (passage 5–6) were collected and incubated with 25 nM of TMRE dye in phosphate-buffered saline (PBS) for 30 min before sorting. TMRE was selected based on studies showing its fast equilibration time, low mitochondrial binding, and almost negligible electron transport chain inhibition if used at concentrations lower than 1 μM.[70] The concentration of 25 nM was chosen to avoid overloading of mitochondria with the dye, which can result in self-quenching due to the formation of dye aggregates.[70] FCCP (carbonyl cyanide 4-(trifluoromethoxy) phenylhydrazone) was used as a positive control for mitochondrial depolarization (Supplementary Fig. S1). Sorting was performed using a BD FACSAria. hMSCs were gated to isolate live cells from dead cells and debris using forward scatter-area (FSC-A) and side scatter-area (SSC-A) channels. Live cells were then gated and sorted into two tubes to obtain two populations: Low 30% and High 10% of TMRE (PE-A channel) signal, labeled as MSC-$\Delta\Psi_L$ and MSC-$\Delta\Psi_H$, respectively. A small aliquot of EE-hMSCs was reanalyzed with flow cytometry to confirm separation of hMSCs postsorting. EE populations were either collected right after sorting or seeded on 24-well plates at a density of 5×10^4 per well and collected after 24 h of culture using 500 μL of lysis buffer (100 mM Tris, 500 mM LiCl, 10 mM EDTA, 1% LiDS, 5 mM dithiothreitol, pH $\sim$7.8). Postsorting analysis was performed using the FlowJo software (TreeStar).

MSC/macrophage activation and coculture

A vial of cryopreserved RAW 264.7 (ATCC) murine macrophages was thawed and expanded in monolayer culture. Macrophages were maintained at 37°C/5% CO_2 in cell culture medium, which consisted of Dulbecco's modified Eagle's medium (DMEM; Corning Cellgro) supplemented with 10% FBS (Hyclone), 100 U/mL penicillin, and 100 μg/mL streptomycin (Gibco). A total of 2.5×10^4 RAW 264.7 (passage 19 from our cryostocks) were plated in 0.4-μm-pore inserts for 12-well transwell plates (Falcon) in 500 μL of activation media (DMEM +10% FBS Premium Select +20 ng/mL IFNγ + 100 ng/mL LPS). To be consistent with macrophage nomenclature, we refer to our activated murine macrophages as M(LPS+IFNγ). After 24 h, 5×10^4 of EE-MSCs were added to the bottom of separate transwell plates in 1 mL of media (DMEM +10% FBS) to achieve a 2:1 MSC:macrophage ratio. This was selected to be consistent and comparable with prior work that assessed immunomodulatory effects of hMSCs on target cell types.[71] After 4 h to allow for hMSCs to settle and attach, media were changed to remove dead cells and debris, and inserts containing M(LPS+IFNγ) were added to the appropriate hMSC wells. Fresh 500 μL of activated media was added into the transwells. After 24 h of coculture, cells were washed with

Dulbecco's Phosphate Buffered Saline (DPBS) and collected using 500 and 250 μL of lysis buffer for MSC and M(LPS+IFNγ), respectively, and then stored at −80°C. The 24-h experimental time point was chosen to assess the phenotype of hMSCs within the expected time frame of *in vivo* homing and therapeutic effects.[72–75]

mRNA extraction and quantitative reverse transcription–polymerase chain reaction

mRNA extraction was performed using Dynabeads mRNA direct kit (Life Technologies).[68] Quantitative reverse transcription–polymerase chain reaction (RT-qPCR) was performed to compare mRNA levels across the various experimental groups using a StepOne Real-Time PCR system and the SuperScript III Platinum One-Step qRT-PCR kit (Life Technologies) according to the manufacturer's instructions. Primers were purchased from Eurofins (Operon) or OriGene, and the sequences are provided in Supplementary Tables S1 and S2. Gene expression was normalized to three reference genes (GAPDH, L32, and β-actin) for hMSCs and L32 for RAW264.7 and normalized across all groups. The choice of normalizers for hMSCs was based on the assumption that plasma and mitochondrial membrane potential differences may affect the expression of multiple housekeeping genes and hence using multiple reference genes may minimize any systematic errors due to normalization. The choice of reference genes for RAW 264.7 was based on relevant literature for macrophages.[76–79] Melting temperature analysis was performed for each reaction to verify the appropriate amplification product, and these values are reported in Supplementary Tables S1 and S2.

Statistical analysis

All results are reported as the mean ± standard error. The sample size, donor number, and number of experiments performed for each figure are reported in their respective legends. To assess relative differences between groups in terms of FACS parameters and mRNA expression, the means of each marker were compared using an independent-sample Student's *t*-test between MSC-$\Delta\Psi_L$ and MSC-$\Delta\Psi_H$ or activated macrophages cocultured with either MSC-$\Delta\Psi_L$ or MSC-$\Delta\Psi_H$. For all tests, a p-value <0.05 was considered significant. Homogeneity of variance was verified using Levene's test. SPSS software and Excel's data analysis tool plugin were utilized to conduct statistical analysis.

Results

Cell enrichment strategy to obtain EE-hMSCs

Populations of hMSCs were EE using TMRE, a lipophilic cationic dye that accumulates in the plasma and mitochondrial matrices depending on the magnitude of the voltage across these membranes. The events were inversely gated to remove dead cells and debris, and subsequently sorted for low 30% and high 10% of TMRE signal (MSC-$\Delta\Psi_L$ and MSC-$\Delta\Psi_H$, respectively; Fig. 1A). The different percentages

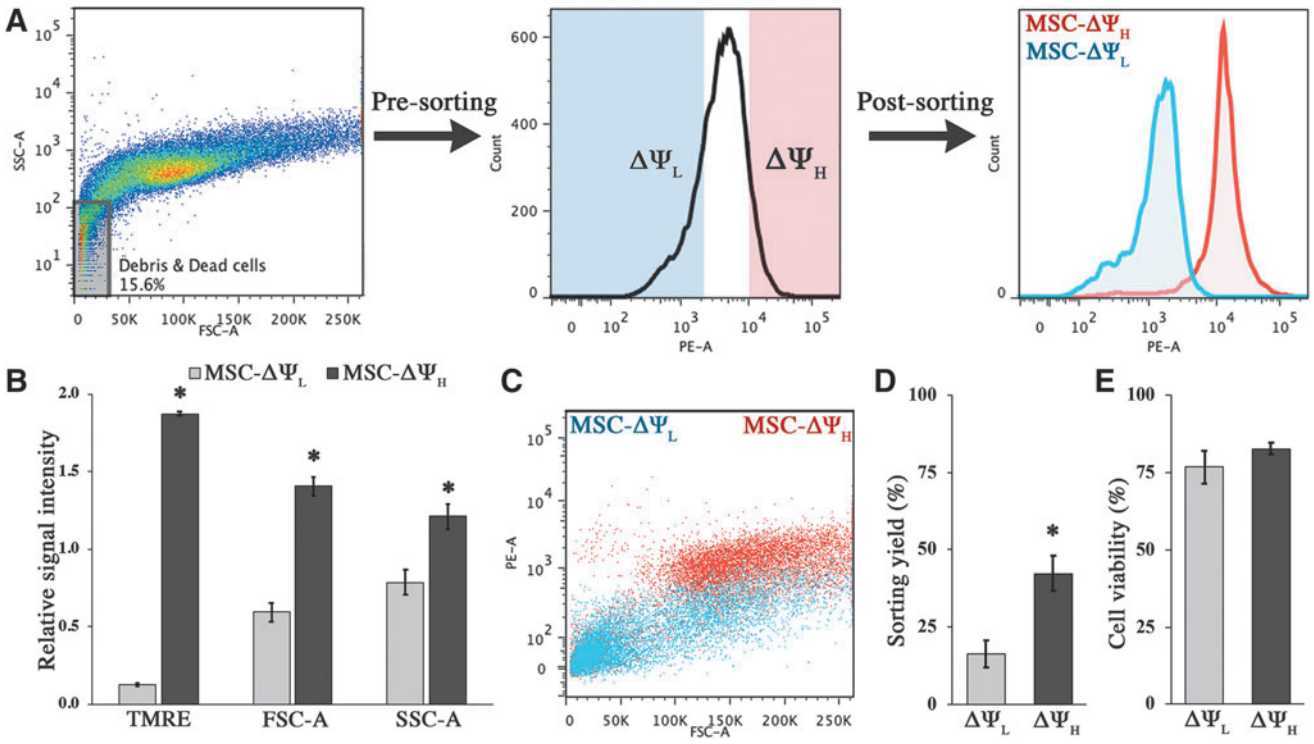

FIG. 1. **(A)** Gating strategy to obtain MSC-$\Delta\Psi_L$ and MSC-$\Delta\Psi_H$ populations. **(B)** Cumulative relative FSC-A, SSC-A, and TMRE intensities across all sorting experiments for MSC-$\Delta\Psi_L$ and MSC-$\Delta\Psi_H$. **(C)** Representative FSC-A versus TMRE dot plot of MSC-$\Delta\Psi_L$ and MSC-$\Delta\Psi_H$. **(D)** Sorting yield (cell count/sorted events) across all sorting experiments. **(E)** Cell viability after sorting as determined by trypan blue. *Denotes difference relative to MSC-$\Delta\Psi_L$, $p<0.05$. Data represent mean ± standard deviation of at least four independent experiments. FSC-A, forward scatter-area; MSC, mesenchymal stem cell; SSC-A, side scatter-area; TMRE, tetramethylrhodamine ethyl ester.

were chosen to achieve large enough TMRE separation after sorting, while maintaining a relatively comparable number of EE-hMSCs after sorting. Overall, across the sorting experiments we performed, postsorting analyses of our populations confirmed that MSC-$\Delta\Psi_H$ had approximately an order of magnitude greater median TMRE signal than MSC-$\Delta\Psi_L$ (15-fold, $p<0.001$, Fig. 1B). MSC-$\Delta\Psi_H$ also had significantly greater median forward scatter signal/cell size (2.4-fold, $p<0.001$, Fig. 1B), and this was confirmed visually using light microscopy. In addition, MSC-$\Delta\Psi_H$ had greater median side scatter signal relative to MSC-$\Delta\Psi_L$ (1.5-fold, $p=0.038$, Fig. 1B), which is an indicator of cell granularity/complexity. Throughout all experiments, we consistently observed a direct relationship between TMRE and FSC-A signal magnitudes (Fig. 1C). In addition to fluorescence and size differences, sorting populations also differed in terms of sorting yield, defined as percentage of cells sorted as determined by an automatic cell counter Eve (NanoEnTek) divided by the number of sorted events detected by FACS. Specifically, sorting yield was significantly lower for MSC-$\Delta\Psi_L$ with a mean yield of 16%, relative to MSC-$\Delta\Psi_H$ with a mean yield of 42% ($p<0.001$, Fig. 1D). At the same time, average viability, assessed by trypan blue staining, between the two EE populations was not statistically different ($p=0.32$, Fig. 1E).

Cumulatively, these results suggested that hMSC populations with distinct TMRE levels and no differences in terms of viability could be obtained, but this was associated with other differential parameters of the cells, including size and granularity.

EE-hMSCs exhibit phenotypical differences with respect to senescence, stemness, autophagy, and immunomodulation

After confirming our ability to sort cells via TMRE staining, we aimed to assess potential phenotypic differences of MSC-$\Delta\Psi_L$ and MSC-$\Delta\Psi_H$ that were persistent across cell donors. HMSCs sorted from three donors were collected immediately after sorting, and gene expression of some of the key markers associated with senescence, stemness (multipotency), immunomodulation, and autophagy was assessed. Postsorting analysis showed that TMRE, FSC-A, and SSC-A signals were greater in the MSC-$\Delta\Psi_H$ group (Fig. 2A), with the most notable difference being detected in EE-hMSCs derived from donor 7071L (Supplementary Fig. S2A). In terms of gene expression for senescence, mRNA levels of cell cycle inhibitor *p21* were significantly lower in MSC-$\Delta\Psi_L$ (1.3-fold, $p=0.001$, Fig. 2B). Conversely, the expression DNA methyltransferase (*DNMT1*), involved in maintenance of self-renewal of MSCs, was significantly upregulated in MSC-$\Delta\Psi_L$ (1.4-fold, $p=0.009$, Fig. 2B). Other senescence-associated lysosomal markers (β-galactosidase, *GLB1*, and α-fucosidase, *FUCA1*) were not statistically different across donors, although in one donor (7071L), they tended to be reduced in MSC-$\Delta\Psi_L$ (Supplementary Fig. S2B).

In terms of stemness markers, mRNA levels of *CD44* (home cell adhesion molecule [HCAM]) and *CD105* (endoglin) were significantly higher in MSC-$\Delta\Psi_L$ relative to MSC-$\Delta\Psi_H$ (1.4-fold, $p<0.001$ and $p=0.009$, respectively, Fig. 2C). In addition, we found that the expression of

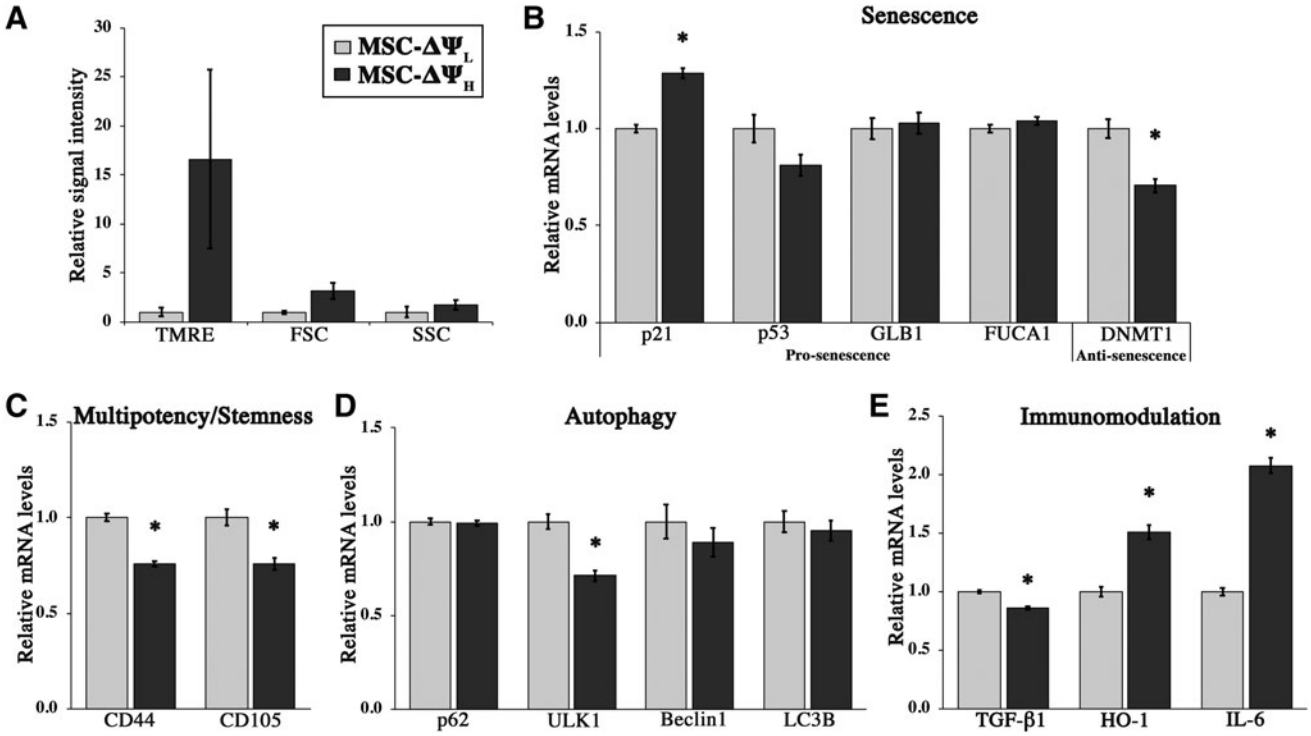

FIG. 2. **(A)** Relative median TMRE, forward and side scatter intensities of EE-hMSCs obtained from three different donors. **(B)** Relative mRNA expression of markers associated with senescence, **(C)** stemness, **(D)** autophagy, and **(E)** immunomodulation from EE-hMSCs collected immediately after FACS from three different donors. *Denotes difference relative to MSC-$\Delta\Psi_L$, $p<0.05$. EE, electrically enriched; FACS, fluorescence-activated cell sorting.

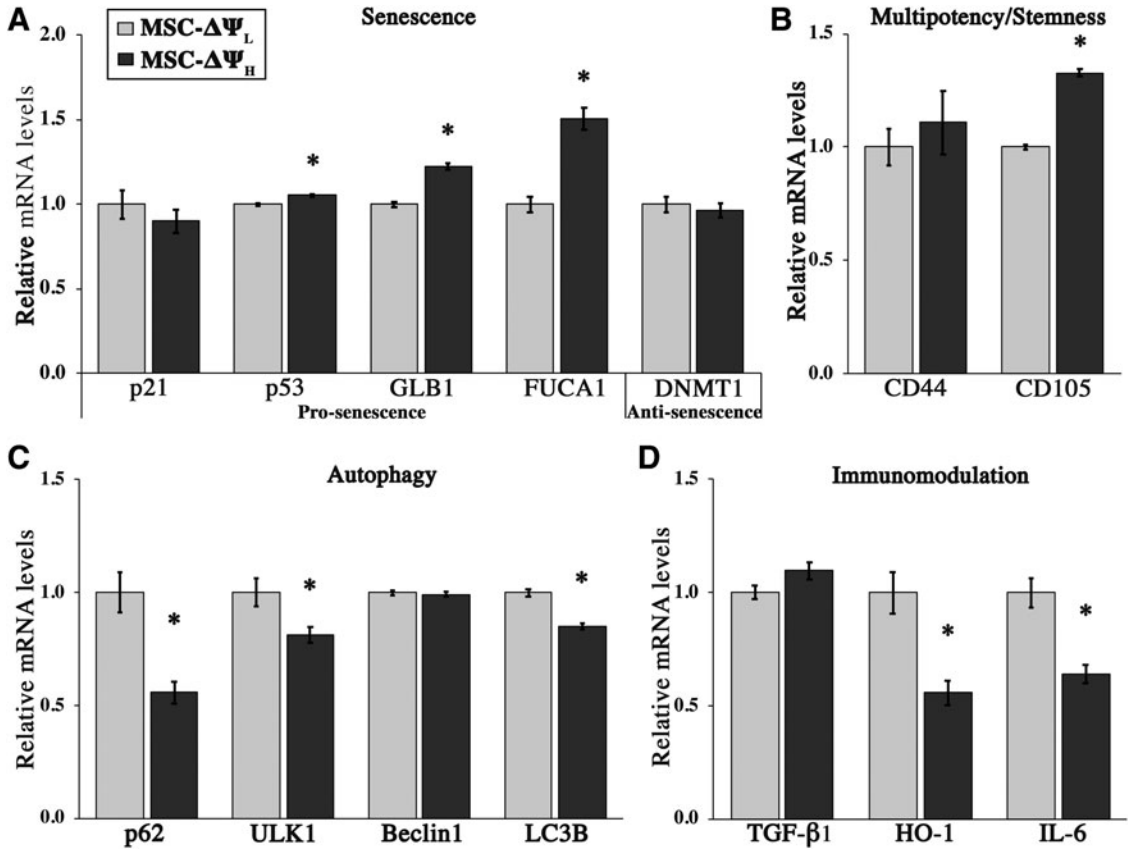

FIG. 3. **(A)** Relative mRNA expression of markers associated with senescence, **(B)** stemness, **(C)** autophagy, and **(D)** immunomodulation from EE-hMSCs collected 24 h after sorting. *Denotes difference relative to MSC-$\Delta\Psi_L$, $p < 0.05$. Data are expressed as mean ± SEM of three independent sorting experiments. SEM, standard error of the mean.

autophagy-related gene *ULK1* was significantly upregulated in MSC-$\Delta\Psi_L$ (1.4-fold, $p = 0.003$, Fig. 2D).

Finally, in terms of immunomodulatory markers, *TGF-β1* was also significantly upregulated in MSC-$\Delta\Psi_L$ relative to MSC-$\Delta\Psi_H$ (1.2-fold, $p = 0.003$, Fig. 2E). In contrast, other prominent MSC-related immunomodulation markers *HO-1/HMOX1* and *IL-6* were significantly decreased in MSC-$\Delta\Psi_L$ (1.5-fold, $p = 0.003$, and 2.1-fold, $p < 0.001$, respectively, Fig. 2E).

Overall, gene expression analyses immediately postsorting suggested that hMSCs with lower TMRE intensity may possess reduced senescence, enhanced stemness, and elevated levels of autophagy. However, immunomodulation profiling revealed a marker-dependent relationship between MSCs sorted via TMRE intensity.

EE-hMSCs are phenotypically different 24 h after electrical enrichment

Given the differences in mRNA expression immediately after the sorting, we asked whether the differences would persist in EE-hMSCs cultured for 24 h after sorting. The sorted cells from the donor with the most consistent mRNA expression in terms of stemness, immunomodulation, and senescence-associated markers were seeded (7071L; Supplementary Fig. S3). In contrast to day 0 analyses, the difference in expression of senescence-associated markers *p21* and *DNMT1* was lost at the 24-h time point. Other senescence-associated lysosomal markers *GLB1* and *FUCA1* were significantly lower in MSC-$\Delta\Psi_L$ relative to MSC-$\Delta\Psi_H$ (1.5-fold, $p < 0.001$, and 1.2-fold, $p = 0.003$, respectively, Fig. 3A).

In terms of stemness markers, there was no difference in *CD44* expression, while significantly lower levels of *CD105* were noted in MSC-$\Delta\Psi_L$ (1.3-fold, $p < 0.001$, Fig. 3B). In contrast, relative to MSC-$\Delta\Psi_H$, MSC-$\Delta\Psi_L$ had significantly increased mRNA levels of the autophagic indicators *p62* (1.8-fold, $p = 0.012$), *ULK1* (1.2-fold, $p = 0.045$), and *LC3B* (1.2-fold, $p = 0.002$; Fig. 3C) in parallel with increases in mRNA levels of immunomodulatory markers *HO-1* (1.8-fold, $p = 0.01$) and *IL-6* (1.6-fold, $p = 0.009$; Fig. 3D). Results for *CD105*, *HO-1*, and *IL-6* were all opposite of what we observed at 0 h.

Cumulatively, these data supported the notion that cells sorted via TMRE intensity remain as distinct cell states even after culture. Moreover, focusing on consistencies between time points suggested that MSC-$\Delta\Psi_L$ exhibit features of reduced senescence and enhanced autophagy. At the same time, acknowledging differences between the two time points highlighted diverging mRNA expression in terms of immunomodulatory markers *HO-1* and *IL-6*, as well as the stemness marker CD105 (Supplementary Fig. S4).

MSC-$\Delta\Psi_L$ suppresses features of M(LPS ± IFNγ) in coculture

To characterize possible functional differences between our two hMSC populations, we evaluated the potential

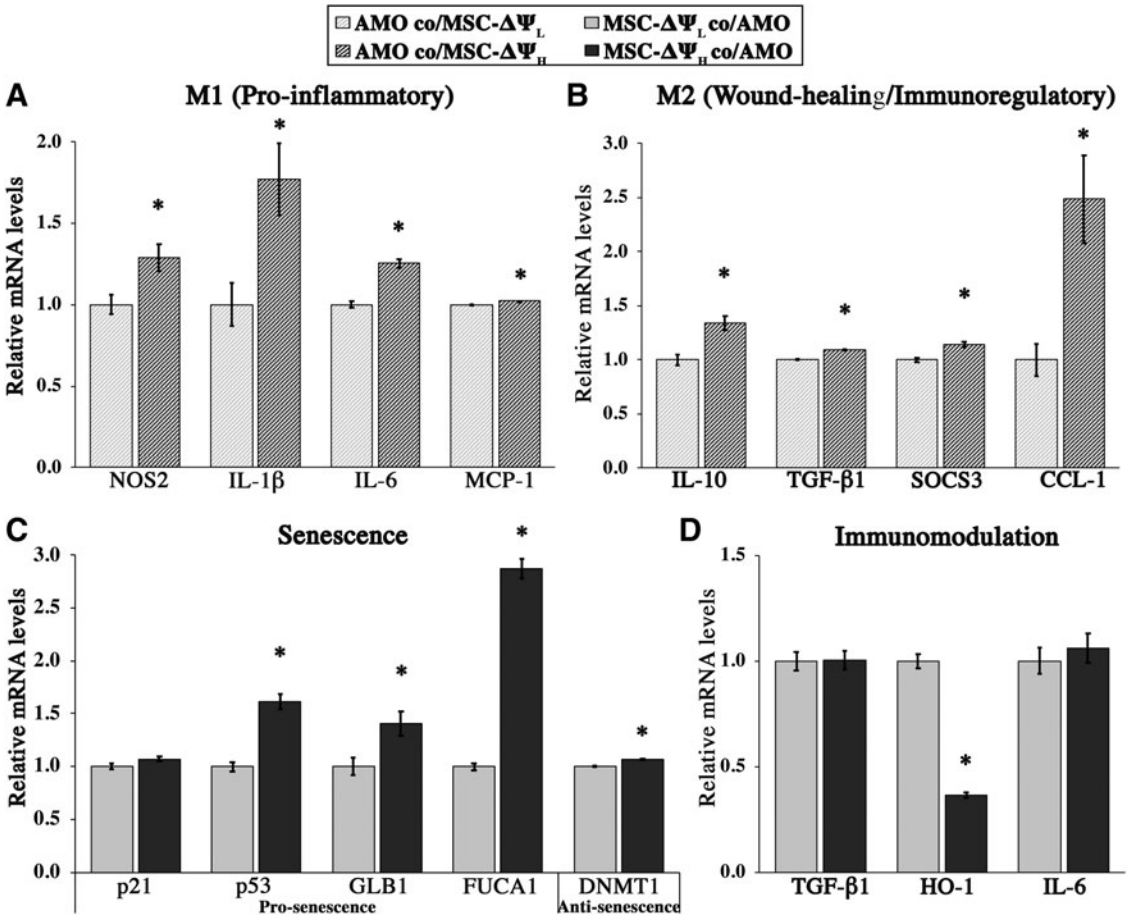

FIG. 4. **(A)** Relative mRNA expression of markers associated with M1 and **(B)** M2 phenotype of activated macrophages after 24 h of coculture with EE-hMSCs. Relative mRNA expression of markers associated with **(C)** senescence and **(D)** immunomodulation in EE-hMSCs cocultured with activated macrophages for 24 h. In **(A, B)**, *denotes difference relative to AMO co/MSC-$\Delta\Psi_L$, $p < 0.05$. In **(C, D)**, *denotes difference relative to MSC-$\Delta\Psi_L$ co/AMO, $p < 0.05$. Data represent mean ± SEM of triplicate samples.

immunosuppressive effect of EE-hMSCs through a coculture with M(LPS+IFNγ). EE-hMSCs were generated using the same gating strategy as in Figure 1, and representative FSC, SSC, and TMRE spectrums postsorting are shown in Supplementary Figure S5. After 24 h of coculture, the mRNA levels of macrophage activation markers were assessed. Relative to MSC-$\Delta\Psi_H$, M(LPS+IFNγ) exposed to MSC-$\Delta\Psi_L$ expressed significantly lower levels of classical proinflammatory (M1) markers *NOS2* (1.3-fold, $p = 0.048$), *IL-1β* (1.8-fold, $p = 0.04$), *IL-6* (1.3-fold, $p = 0.002$), and *MCP-1/CCL-2* (1.02-fold, $p < 0.001$, Fig. 4A). In addition to ''M1'' markers, MSC-$\Delta\Psi_L$ also decreased the expression of markers typically associated with the ''M2'' state, such as *IL-10* (1.3-fold, $p = 0.01$), *CCL-1* (2.5-fold, $p = 0.026$), *TGF-β1* (1.1-fold, $p < 0.001$), and *SOCS3* (1.1-fold, $p = 0.014$, Fig. 4B).

To gain insight into the differences noted in M(LPS+IFNγ), we also profiled the phenotype of EE-hMSCs from the coculture via mRNA expression of senescence and immunomodulatory markers. Consistent with the 24-h monoculture results (Fig. 3), the expressions of senescence-associated markers *p53* (1.6-fold, $p < 0.001$), *GLB1* (1.4-fold, $p = 0.04$), and *FUCA1* (2.9-fold, $p < 0.001$) were all significantly lower in MSC-$\Delta\Psi_L$ (Fig. 4C). The lower levels of senescence-associated markers were also associated with differential expression of the immunomodulatory marker *HO-1*. Specifically, *HO-1* mRNA levels were elevated in MSC-$\Delta\Psi_L$ population (2.8-fold, $p < 0.001$) while levels of *IL-6* and *TGF-β1* were similar between the two groups (Fig. 4D). These EE-hMSC results were also relatively consistent with what was observed in monoculture.

Taken together, these results suggested that MSC-$\Delta\Psi_L$ may suppress the expression of genes associated with macrophage activation, and this response may be mediated, in part, by *HO-1*.

Discussion

Our long-term goal is to develop an enrichment strategy for specific stem cell populations with reduced senescence and enhanced stemness, potentially resulting in greater immunomodulatory and regenerative capacity of hMSCs. We envision that electrical enrichment may be implemented as a novel and complementary technology/concept for hMSC therapy. In this study, we sought to initially develop the idea of exploiting hMSC electrical properties, such as plasma and mitochondrial membrane potentials, which we and others have hypothesized to be associated with distinct cell states and functions.[26,27,38,40–46] Specifically, our goals were to begin to (i) develop a protocol to

achieve EE-hMSCs with distinct electrical states through FACS TMRE intensity sorting, and (ii) assess the potential relationship with respect to EE-hMSC state and function. Both the idea to sort hMSCs based on electrical properties and the combination of metrics/processes analyzed (autophagy, immunomodulation, multipotency/stemness, and senescence) to describe the stem cells are novel. Therefore, our discussion first focuses on technical considerations and observations followed by those of biological nature.

Cell enrichment based on TMRE yielded two distinct stem cell subpopulations—MSC-$\Delta\Psi_L$ and MSC-$\Delta\Psi_H$—characterized by an order of magnitude difference in signal intensity postsorting, suggesting successful acquisition of distinct electrical properties. Interestingly, MSC-$\Delta\Psi_H$ also exhibited a significantly larger cell size and granularity. Given the similarities between TMRE and FSC intensities, cell enrichment based on FSC may present an alternative, simpler strategy for stem cell enrichment in future work.

We are unable to compare the associations between TMRE, FSC, and SSC with others who have performed similar sorting experiments in other cell types because FSC and SSC parameters were not reported.[28,31,33,36] Despite being commonly omitted, it is appropriate to comment on how these parameters may change the interpretation of fluorescence as they relate to voltage. For example, the greater size of MSC-$\Delta\Psi_H$ is likely not a major confounding element based on previous experimental and computational work that measures or simulates fluorescence in response to cell and/or mitochondrial volume manipulations.[80,81] In other words, Nernstian dyes can be cell volume insensitive, and thus, size may not be a major contributor to fluorescence intensity, likely because of the binding nature of the dyes to membranes. It remains a possibility that differential SSC signals, a potential indication of mitochondrial content differences,[82] in EE-hMSCs could account for fluorescence differences between our sorted populations. Unfortunately, correcting for mitochondrial volume fraction, a known contributor to tetramethylrhodamine signal intensity, is technically challenging,[80] especially in light of recent results questioning the use of mitochondrial tracker dyes for mitochondrial mass assessment.[83] In addition, we are unable to establish specifically whether differences in TMRE levels between MSC-$\Delta\Psi_L$ and MSC-$\Delta\Psi_H$ populations are due to the mitochondrial or plasma membrane potentials as both are known contributors to TMRE signal.[80,84] These and other limitations of voltage-sensitive dye utilization (including accounting for apparent activity coefficients and apparent charge of TMRE) prevent us from definitively claiming that our populations are indeed distinct electrically based solely on fluorescence intensity comparisons, but we are able to assume so with a degree of confidence, as is done ubiquitously in the literature.[28,31,33,36,58,59]

One of the main challenges we faced during our experiments was the sorting yield (the percentage of live cells as counted by cell counter or hematocytometer over sorted events registered by FACS). We found that while yield varied between experiments for both populations, it was consistently lower for MSC-$\Delta\Psi_L$ (5–30%) compared with MSC-$\Delta\Psi_H$ (25–65%) subpopulations. We have no definitive explanation for this result, but possibilities include technical limitations of FACS sorting of lower intensity signals or a differential capacity to handle sorting stresses between EE-MSC populations. The cell recovery and other problems we encountered might be improved through sorting and collecting hMSCs in medium containing some nutrients,[85] and/or by adjusting technical parameters of FACS (i.e., sheath pressure, nozzle size, and sorting speed).

After generating EE-hMSCs with a degree of confidence, we asked whether these populations varied with respect to phenotypic and functional measures with the hypothesis that the MSC-$\Delta\Psi_L$ population would exhibit features of reduced senescence with concomitant increases in stemness and immunomodulatory properties. In partial support for these relationships, we observed lower levels of the ''prosenescence''[86–88] descriptors FSC, SSC, and *p21* mRNA, and higher levels of the ''antisenescence''[89,90] *DNMT1* marker in all three donors at time zero (Fig. 2B), and lower levels of ''prosenescence''[91–93] markers *p53*, *GLB1*, and *FUCA1* 24 h postsorting (Fig. 3A) in the MSC-$\Delta\Psi_L$ population. Although distinct from senescence, autophagy pathways have been shown to prevent senescence in aging muscle stem cells in a mouse model by decreasing p16 and H2AX expression, as well as reducing senescence-associated β-galactosidase activity.[94] In line with this idea, we found that MSCs-$\Delta\Psi_L$ had greater expression of autophagic marker *ULK1* right after sorting (Fig. 2D) and increased expression of *p62*, *ULK1*, and *LC3B* at 24 h (Fig. 3C).

Even though specific senescence and autophagy markers may have switched between time points, at no point did we observe evidence to the contrary. Cumulatively, these data are consistent with the notion that MSC-$\Delta\Psi_L$ are in a state characterized by reduced senescence and enhanced autophagy relative to MSC-$\Delta\Psi_H$. The mechanistic links between $\Delta\Psi_m$ and hMSC state and function are poorly understood but potentially numerous.[26–55] Focusing on the mitochondria as one example: $\Delta\Psi_m$ has been suggested not only to directly communicate with the nucleus to regulate gene expression[26] but also $\Delta\Psi_m$ is an integration point for many processes of cell metabolism,[95] regulating mitochondrial reactive oxygen species,[96,97] mitochondrial respiration, and ATP synthesis.[98] Each metabolic parameter in turn is associated with a range of downstream effects, resulting in complex and incompletely understood systems-level interconnections that render cause/effect relationships difficult to tease out.

As separate but related to senescence and autophagy, it is also useful to assess the expression of stemness (or multipotency) markers. Typically, these MSC markers, such as *CD44* (*HCAM*) and *CD105* (*endoglin*), are known to decline with aging[87] and differentiation.[99–101] Both surface marker mRNA levels were elevated in MSC-$\Delta\Psi_L$ in all three donors (Fig. 2C), suggesting enhanced stemness in MSC-$\Delta\Psi_L$, consistent with not only our hypothesis but also the general perception that MSCs with reduced senescence have greater stemness. However, once seeded and cultured for 24 h, phenotypic shifts were observed (Supplementary Fig. S4). MSC-$\Delta\Psi_L$ exhibited lower levels of CD105 in comparison with MSC-$\Delta\Psi_H$, this switch contrasts that of the senescence markers that cumulatively suggested a consistent senescent state. We have no explanation for this finding, but the data lend credence to the notion that stemness and senescence may be distinct processes with disparate functions.

The relationship between the stemness and immunomodulatory properties still remains controversial with opposing findings present in literature.[102,103] The preservation of

stemness remains one of the priorities in many *in vitro* investigations with the assumption that a more stem-like state correlates with better therapeutic immunomodulation. We found that MSC-$\Delta\Psi_H$ had elevated mRNA expression of HO-1, a rate-limiting enzyme in heme metabolism, with anti-inflammatory, antioxidative, and antiapoptotic functions,[104,105] as well as pleiotropic cytokine IL-6, which is heavily involved in the immunomodulatory function of MSCs. However, after 24 h of culture of EE-hMSCs, we observed a shift toward greater expression of *HO-1* and *IL-6* in MSC-$\Delta\Psi_L$. This shift in immunomodulatory markers coincided with a shift in opposing direction of *CD105*, a pattern that compares favorably with findings from Sempere et al.[106] Specifically, they described populations of adipose-derived stem cells with low expression of CD105, yet greater IL-4 expression and a more inhibitory effect on lymphocyte proliferation, while MSCs with highly expressed CD105 secreted more proinflammatory cytokine IL-1β.[106] Together, these data suggest that the relationship between stemness and immunomodulation is not straightforward. Unfortunately, making definitive conclusions about stemness and immunomodulation/therapeutic efficacy is difficult due to the complexity of these processes, and the fact that both studies assessed a limited marker set.

While we observed complex, marker-dependent phenotypic shifts of EE-hMSCs after culturing for 24 h, the two populations were still distinct. To help improve clarity, we tested their immunomodulation capacity by coculture with M(LPS+IFNγ). Since we observed that MSC-$\Delta\Psi_L$ was able to downregulate both M1 and M2 markers, we are not able to say that MSC-$\Delta\Psi_L$ induced an M2-like transition, a common finding when investigating MSC effects on macrophages.[107] Given that both M1 and M2 markers are associated with pathologies,[108] the overall downregulation of inflammation-related genes may suggest that MSC-$\Delta\Psi_L$ may have stronger immunosuppressive effect relative to MSC-$\Delta\Psi_H$. Profiling the EE-hMSCs from the coculture revealed a marked increase of *HO-1* in MSC-$\Delta\Psi_L$, suggesting that effects on macrophages may be driven, in part, by higher expression of *HO-1*. This is supported by several lines of *in vitro* and *in vivo* data demonstrating the impact of HO-1 on reduction of the proinflammatory phenotype of stimulated macrophages,[109–112] and specifically HO-1 derived from hMSCs.[113] In our study, MSC-$\Delta\Psi_H$ had greater expression of senescence-associated markers and reduced immunomodulatory markers *HO-1* (and *IL-6* in monoculture). These findings are consistent with reports that senescent MSCs display reduced immunomodulatory capacity.[19] The effects of EE-hMSCs on activated macrophages are more closely associated with the phenotype of EE-hMSCs 24 h after coculture, rather than immediately after sorting.

Some limitations of our study must be taken into account when interpreting the results, aside from those relating to dye staining mentioned earlier. Our study was largely proof-of-concept in nature, so we were limited with respect to many of the analyses and types of experimental groups included. For example, the analysis of EE-hMSCs was only performed utilizing mRNA levels. Owing to technical limitations of FACS, the number of available cells is a limiting factor for protein expression analysis, as mentioned earlier. This is particularly a limitation for making claims regarding a metabolic process such as autophagy, where definitive flux information cannot be deduced from mRNA levels. Second, the study could have benefited from a comparison with cells that were expanded but not subjected to any enrichment. Third, within the scope of this work, we decided to restrict the assessment of EE-hMSCs to specific passage numbers (5–6) and time points (0 and 24 h). Finally, while we were relatively extensive in our selection of processes and marker sets, we were by no means exhaustive. As we develop our knowledge of the enrichment process, deeper interrogation of cell state with functional, protein, metabolite, and electrophysiological analyses coupled with gold standard comparisons will be the focus of future work. As a separate focus, we will pursue ionic and electrical manipulations during expansion of hMSCs to induce bioelectrical states associated with enhanced immunomodulatory/regenerative capacity.

Conclusions

We demonstrated that hMSCs can be enriched based on TMRE staining into two distinct populations—MSC-$\Delta\Psi_L$ and MSC-$\Delta\Psi_H$, likely reflecting differences in basal electrical states of these populations. Phenotypical differences were observed both immediately and 24 h after enrichment. While many phenotypic markers switched or changed pattern during this period, MSC-$\Delta\Psi_L$ tended to express lower levels of senescence-associated markers, and greater expression of autophagy markers. Subsequent culture of EE-hMSCs with M(LPS+IFNγ) suggested that this population exhibits a more overall immunosuppressive potential. Cumulatively, our results deepen our understanding of hMSC state and suggest that future work developing EE-hMSCs is warranted.

Authors' Contributions

J.E.M. conceived the project. J.E.M. and M.S.H. designed the experiments. T.K. performed experiments and data collection. J.E.M., M.S.H., and T.K. analyzed and interpreted data. J.E.M. and T.K. wrote the manuscript. M.S.H., M.L., and D.L.K. revised and edited the manuscript. All authors have reviewed and approved the manuscript before submission.

The authors declare that the manuscript has not been published, in press, or submitted elsewhere.

Author Disclosure Statement

The authors declare the following potential conflict of interest with respect to the research, authorship, and/or publication of this article: T.K., J.E.M., and M.H. have a provisional patent (U.S Provisional Patent, Application No. 62/889,285) for this work.

Funding Information

The authors thank the National Institutes of Health (P41 Resource Center on Tissue Engineering [P41EB002520] to D.L.K., NIA R03AG064550 and NIA R03AG056168 to M.H., NIMH F32MH118678 to J.E.M., and NIGMS 5T32GM067545-13 to T.K.) and the Paul G. Allen Foundation (# 2171), to D.L.K. and M.L., for funding.

Supplementary Material

Supplementary Table S1
Supplementary Table S2

Supplementary Figure S1
Supplementary Figure S2
Supplementary Figure S3
Supplementary Figure S4
Supplementary Figure S5

References

1. Le Blanc K, Mougiakakos D. Multipotent mesenchymal stromal cells and the innate immune system. Nat Rev Immunol 2012;12:383–396.
2. Liu ZJ, Zhuge Y, Velazquez OC. Trafficking and differentiation of mesenchymal stem cells. J Cell Biochem 2009;106:984–991.
3. Tyndall A. Successes and failures of stem cell transplantation in autoimmune diseases. Hematology Am Soc Hematol Educ Program 2011;2011:280–284 .
4. Malliaras K, Kreke M, Marbán E. The stuttering progress of cell therapy for heart disease. Clin Pharmacol Ther 2011;90:532–541.
5. Xia P, Wang X, Lin Q, et al. Efficacy of mesenchymal stem cells injection for the management of knee osteoarthritis: A systematic review and meta-analysis. Int Orthop 2015;39:2363–2372.
6. Koh YG, Jo SB, Kwon OR, et al. Mesenchymal stem cell injections improve symptoms of knee osteoarthritis. Arthroscopy 2013;29:748–755.
7. Mastri M, Lin H, Lee T. Enhancing the efficacy of mesenchymal stem cell therapy. World J Stem Cells 2014;6: 82–93.
8. Connick P, Kolappan M, Crawley C, et al. Autologous mesenchymal stem cells for the treatment of secondary progressive multiple sclerosis: An open-label phase 2a proof-of-concept study. Lancet Neurol 2012;11:150–156.
9. Hare JM, Traverse JH, Henry TD, et al. A randomized, double-blind, placebo-controlled, dose-escalation study of intravenous adult human mesenchymal stem cells (prochymal) after acute myocardial infarction. J Am Coll Cardiol 2009;54:2277–2286.
10. Jiang R, Han Z, Zhuo G, et al. Transplantation of placenta-derived mesenchymal stem cells in type 2 diabetes: A pilot study. Front Med China 2011;5:94–100.
11. Tan J, Wu W, Xu X, et al. Induction therapy with autologous mesenchymal stem cells in living-related kidney transplants: A randomized controlled trial. JAMA 2012; 307:1169–1177.
12. Kuzmina LA, Petinati NA, Parovichnikova EN, et al. Multipotent mesenchymal stromal cells for the prophylaxis of acute graft-versus-host disease-A phase II study. Stem Cells Int 2012;2012:968213. DOI: 10.1155/2012/968213.
13. Li J, Wong WH, Chan S, et al. Factors affecting mesenchymal stromal cells yield from bone marrow aspiration. Chin J Cancer Res 2011;23:43–48.
14. Ringdén O, Uzunel M, Rasmusson I, et al. Mesenchymal stem cells for treatment of therapy-resistant graft-versus-host disease. Transplantation 2006;81:1390–1397.
15. Arima N, Nakamura F, Fukunaga A, et al. Single intra-arterial injection of mesenchymal stromal cells for treatment of steroid-refractory acute graft-versus-host disease: A pilot study. Cytotherapy 2010;12:265–268.
16. Martin I, De Boer J, Sensebe L. A relativity concept in mesenchymal stromal cell manufacturing. Cytotherapy 2016;18:613–620.
17. Li Z, Liu C, Xie Z, et al. Epigenetic dysregulation in mesenchymal stem cell aging and spontaneous differentiation. PLoS One 2011;6:e20526.
18. Alves H, Munoz-Najar U, De Wit J, et al. A link between the accumulation of DNA damage and loss of multipotency of human mesenchymal stromal cells. J Cell Mol Med 2010;14:2729–2738.
19. Li X-Y, Ding J, Zheng ZH, et al. Long-term culture in vitro impairs the immunosuppressive activity of mesenchymal stem cells on T cells. Mol Med Rep 2012;6:1183–1189.
20. Phinney DG, Sensebe L. Mesenchymal stromal cells: Misconceptions and evolving concepts. Cytotherapy 2013; 15:140–145.
21. Lee WC, Shi H, Poon Z, et al. Multivariate biophysical markers predictive of mesenchymal stromal cell multipotency. Proc Natl Acad Sci U S A 2014;111:E4409–E4418.
22. Whitfield MJ, Lee WCJ, Van Vliet KJ. Onset of heterogeneity in culture-expanded bone marrow stromal cells. Stem Cell Res 2013;11:1365–1377.
23. Rennerfeldt DA, Van Vliet KJ. Concise review: When colonies are not clones: Evidence and implications of intracolony heterogeneity in mesenchymal stem cells. Stem Cells 2016;34:1135–1141.
24. Liu Y, Munoz N, Bunnell BA, et al. Density-dependent metabolic heterogeneity in human mesenchymal stem cells. Stem Cells 2015;33:3368–3381.
25. Martínez-Peinado P, Pascual-García S, Roche E, et al. Differences of clonogenic mesenchymal stem cells on immunomodulation of lymphocyte subsets. J Immunol Res 2018;2018:7232717.
26. Sanin DE, Matsushita M, Klein Geltink RI, et al. Mitochondrial membrane potential regulates nuclear gene expression in macrophages exposed to prostaglandin E2. Immunity 2018;49:1021–1033.e6.
27. Erndt-Marino J, Diaz-Rodriguez P, Hahn MS. Initial in vitro development of a potassium-based intra-articular injection for osteoarthritis. Tissue EngPart A 2018;24: 1390–1392.
28. Sukumar M, Liu J, Mehta GU, et al. Mitochondrial membrane potential identifies cells with enhanced stemness for cellular therapy. Cell Metab 2016;23:63–76
29. Erndt-Marino J, Trinkle E, Hahn MS. Hyperosmolar potassium (K+) treatment suppresses osteoarthritic chondrocyte catabolic and inflammatory protein production in a 3-dimensional in vitro model. Cartilage 2019;10:186–195. DOI: 10.1177/1947603517734028.
30. Kravchenko IV, Furalyov VA, Popov VO. Potassium chloride released from contracting skeletal muscle may stimulate development of its hypertrophy. Biochem Biophys Rep 2019;18:100627.
31. Liu H, He Z, April SL, et al. Biochemical re-programming of human dermal stem cells to neurons by increasing mitochondrial membrane potential. Cell Death Differ 2019;26:1048–1061. DOI: 10.1038/s41418-018-0182-8.
32. Zhang L, Marsboom G, Glick D, et al. Bioenergetic shifts during transitions between stem cell states (2013 Grover Conference series). Pulm Circ 2014;4:387–394.
33. Schieke SM, Ma M, Cao L, et al. Mitochondrial metabolism modulates differentiation and teratoma formation capacity in mouse embryonic stem cells. J Biol Chem 2008;283:28506–28512.
34. Neubert P, Schröder A, Müller DN, et al. Interplay of Na+ balance and immunobiology of dendritic cells. Front Immunol 2019;10:599.

35. Simsek T, Kocabas F, Zheng J, et al. The distinct metabolic profile of hematopoietic stem cells reflects their location in a hypoxic niche. Cell Stem Cell 2010;7:380–390.
36. Vannini N, Girotra M, Naveiras O, et al. Specification of haematopoietic stem cell fate via modulation of mitochondrial activity. Nat Commun 2016;7:13125.
37. Yang W, Nagasawa K, Münch C, et al. Mitochondrial sirtuin network reveals dynamic SIRT3-dependent deacetylation in response to membrane depolarization. Cell 2016;167:985–1000.e21.
38. Zhang WC, Zheng XJ, Du LJ, et al. High salt primes a specific activation state of macrophages, M(Na). Cell Res 2015;25:893–910.
39. Martínez-Reyes I, Diebold LP, Kong H, et al. TCA cycle and mitochondrial membrane potential are necessary for diverse biological functions. Mol Cell 2016;61:199–209.
40. Binger KJ, Gebhardt M, Heinig M, et al. High salt reduces the activation of IL-4- and IL-13-stimulated macrophages. J Clin Invest 2015;125:4223–4238.
41. Girouard H, Bonev AD, Hannah RM, et al. Astrocytic endfoot Ca 2+ and BK channels determine both arteriolar dilation and constriction. Proc Natl Acad Sci U S A 2010;107:3811–3816.
42. Untiet V, Kovermann P, Gerkau NJ, et al. Glutamate transporter-associated anion channels adjust intracellular chloride concentrations during glial maturation. Glia 2017;65:388–400.
43. Vitali I, Fièvre S, Telley L, et al. Progenitor hyperpolarization regulates the sequential generation of neuronal subtypes in the developing neocortex. Cell 2018;174:1264–1276.e15.
44. Matthias J, Maul J, Noster R, et al. Sodium chloride is an ionic checkpoint for human Th2 cell responses and shapes the atopic skin microenvironment. Sci Transl Med 2019;11:pii: eaau0683.
45. Hernandez AL, Kitz A, Wu C, et al. Sodium chloride inhibits the suppressive function of FOXP3 + regulatory T cells. J Clin Invest 2015;125:4212–4222.
46. Eil R, Vodnala SK, Clever D, et al. Ionic immune suppression within the tumour microenvironment limits T cell effector function. Nature 2016;537:539–543.
47. Sundelacruz S, Levin M, Kaplan DL. Membrane potential controls adipogenic and osteogenic differentiation of mesenchymal stem cells. PLoS One 2008;3:e3737.
48. Sundelacruz S, Li C, Choi YJ, et al. Bioelectric modulation of wound healing in a 3D invitro model of tissue-engineered bone. Biomaterials 2013;34:6695–6705.
49. Sundelacruz S, Levin M, Kaplan DL. Role of membrane potential in the regulation of cell proliferation and differentiation. Stem Cell Rev Rep 2009;5:231–246.
50. Li C, Levin M, Kaplan DL. Bioelectric modulation of macrophage polarization. Sci Rep 2016;21044. DOI: 10.1038/srep21044.
51. Levin M. Molecular bioelectricity: How endogenous voltage potentials control cell behavior and instruct pattern regulation in vivo. Mol Biol Cell 2014;25:3835–3850.
52. Sundelacruz S, Levin M, Kaplan DL. Comparison of the depolarization response of human mesenchymal stem cells from different donors. Sci Rep 2015;5:18279.
53. Levin M, Stevenson C. Regulation of cell behavior and tissue patterning by bioelectrical signals: Challenges and opportunities for biomedical engineering. Annu Rev Biomed Eng 2012;14:295–323.
54. Mathews J, Levin M. The body electric 2.0: Recent advances in developmental bioelectricity for regenerative and synthetic bioengineering. Curr Opin Biotechnol 2018;52:134–144.
55. McLaughlin KA, Levin M. Bioelectric signaling in regeneration: Mechanisms of ionic controls of growth and form. Dev Biol 2018;433:177–189.
56. Sundelacruz S, Levin M, Kaplan DL. Depolarization alters phenotype, maintains plasticity of pre-differentiated mesenchymal stem cells. Tissue Eng Part A 2013;19:1889–1908.
57. Pietilä M, Lehtonen S, Närhi M, et al. Mitochondrial function determines the viability and osteogenic potency of human mesenchymal stem cells. Tissue Eng Part C Methods 2009;16:435–445.
58. Tsai A-C, Liu Y, Yuan X, et al. Compaction, fusion, and functional activation of three-dimensional human mesenchymal stem cell aggregate. Tissue Eng Part A 2015;21:1705–1719.
59. Liu Y, Munoz N, Tsai A-C, et al. Metabolic reconfiguration supports reacquisition of primitive phenotype in human mesenchymal stem cell aggregates. Stem Cells 2016;35:398–410.
60. Cesarz Z, Tamama K. Spheroid culture of mesenchymal stem cells. Stem Cells Int 2016;2016.
61. Petrenko Y, Syková E, Kubinová Š. The therapeutic potential of three-dimensional multipotent mesenchymal stromal cell spheroids. Stem Cell Res Ther 2017;8:94.
62. Bartosh TJ, Ylöstalo JH, Mohammadipoor A, et al. Aggregation of human mesenchymal stromal cells (MSCs) into 3D spheroids enhances their anti-inflammatory properties. Proc Natl Acad Sci U S A 2010;107:13724–13729.
63. Ylöstalo JH, Bartosh TJ, Coble K, et al. Human mesenchymal stem/stromal cells cultured as spheroids are self-activated to produce prostaglandin E2 that directs stimulated macrophages into an anti-inflammatory phenotype. Stem Cells 2012;30:2283–2296.
64. Suto EG, Mabuchi Y, Suzuki N, et al. Prospectively isolated mesenchymal stem/stromal cells are enriched in the CD73+ population and exhibit efficacy after transplantation. Sci Rep 2017;7:4838.
65. Cuthbert RJ, Giannoudis PV, Wang XN, et al. Examining the feasibility of clinical grade CD271+ enrichment of mesenchymal stromal cells for bone regeneration. PLoS One 2015;10:e0117855.
66. Poon Z, Lee WC, Guan G, et al. Bone marrow regeneration promoted by biophysically sorted osteoprogenitors from mesenchymal stromal cells. Stem Cells Transl Med 2015;4:56–65.
67. Li H, Ghazanfari R, Zacharaki D, et al. Low/negative expression of PDGFR-α identifies the candidate primary mesenchymal stromal cells in adult human bone marrow. Stem Cell Rep 2014;3:965–974.
68. Diaz-Rodriguez P, Erndt-Marino J, Chen H, et al. A bioengineered in vitro osteoarthritis model with tunable inflammatory environments indicates context-dependent therapeutic potential of human mesenchymal stem cells. Regen Eng Transl Med 2019;5:297–307. DOI: 10.1007/s40883-019-00109-2.
69. Jiang T, Xu G, Wang Q, et al. In vitro expansion impaired the stemness of early passage mesenchymal stem cells for treatment of cartilage defects. Cell Death Dis 2017;8:e2851.

70. Perry SW, Norman JP, Barbieri J, et al. Mitochondrial membrane potential probes and the proton gradient: A practical usage guide. Biotechniques 2011;50:98–115.
71. Stucky EC, Erndt-Marino J, Schloss RS, et al. Prostaglandin E 2 produced by alginate-encapsulated mesenchymal stromal cells modulates the astrocyte inflammatory response. Nano Life 2017;07:1750005.
72. Parekkadan B, Milwid JM. Mesenchymal stem cells as therapeutics. Annu Rev Biomed Eng 2010;12:87–117.
73. Kyriakou C, Rabin N, Pizzey A, et al. Factors that influence short-term homing of human bone marrow-derived mesenchymal stem cells in a xenogeneic animal model. Haematologica 2008;93:1457–1465.
74. Schlosser K, Wang JP, Dos Santos C, et al. Effects of mesenchymal stem cell treatment on systemic cytokine levels in a phase 1 dose escalation safety trial of septic shock patients. Crit Care Med 2019;47:918–925.
75. Németh K, Leelahavanichkul A, Yuen PS, et al. Bone marrow stromal cells attenuate sepsis via prostaglandin E2–dependent reprogramming of host macrophages to increase their interleukin-10 production. Nat Med 2009; 15:42–49.
76. Kriegova E, Arakelyan A, Fillerova R, et al. PSMB2 and RPL32 are suitable denominators to normalize gene expression profiles in bronchoalveolar cells. BMC Mol Biol 2008;9:69.
77. Tanaka A, To J, O'Brien B, et al. Selection of reliable reference genes for the normalisation of gene expression levels following time course LPS stimulation of murine bone marrow derived macrophages. BMC Immunol 2017; 18:1–12.
78. Selvey S, Thompson EW, Matthaei K, et al. β-Actin—An unsuitable internal control for RT-PCR. Mol Cell Probes 2001;15:307–311.
79. Glare EM, Divjak M, Bailey MJ, et al. β-Actin and GAPDH housekeeping gene expression in asthmatic airways is variable and not suitable for normalising mRNA levels. Thorax 2002;57:765–770.
80. Gerencser AA, Chinopoulos C, Birket MJ, et al. Quantitative measurement of mitochondrial membrane potential in cultured cells: Calcium-induced de- and hyperpolarization of neuronal mitochondria. J Physiol 2012;590: 2845–2871.
81. Klapperstück T, Glanz D, Klapperstück M, et al. Methodological aspects of measuring absolute values of membrane potential in human cells by flow cytometry. Cytometry A 2009;75:593–608.
82. Saunders JE, Beeson CC, Schnellmann RG. Characterization of functionally distinct mitochondrial subpopulations. J Bioenerg Biomembr 2013;45:87–99.
83. de Almeida MJ, Luchsinger LL, Corrigan DJ, et al. Dye-independent methods reveal elevated mitochondrial mass in hematopoietic stem cells. Cell Stem Cell 2017;21:725–729.e4.
84. Gerencser AA, Brand MD. Exploiting mitochondria in vivo as chemical reaction chambers dependent on membrane potential. Mol Cell 2016;61:642–643.
85. Emre N, Vidal JG, Elia J, et al. The ROCK inhibitor Y-27632 improves recovery of human embryonic stem cells after fluorescence-activated cell sorting with multiple cell surface markers. PLoS One 2010;5:e12148.
86. Bertolo A, Baur M, Guerrero J, et al. Autofluorescence is a reliable in vitro marker of cellular senescence in human mesenchymal stromal cells. Sci Rep 2019;9:2074.
87. Wagner W, Horn P, Castoldi M, et al. Replicative senescence of mesenchymal stem cells: A continuous and organized process. PLoS One 2008;3:e2213.
88. Stein GH, Drullinger LF, Soulard A, et al. Differential roles for cyclin-dependent kinase inhibitors p21 and p16 in the mechanisms of senescence and differentiation in human fibroblasts. Mol Cell Biol 2015;19:2109–2117.
89. Lin SP, Chiu FY, Wang Y, et al. RB maintains quiescence and prevents premature senescence through upregulation of DNMT1 in mesenchymal stromal cells. Stem Cell Rep 2014;3:975–986.
90. Tsai CC, Pei-Fen S, Yi-Feng H, et al. Oct4 and Nanog directly regulate Dnmt1 to maintain self-renewal and undifferentiated state in mesenchymal stem cells. Mol Cell 2012;47:169–182.
91. Lee BY, Han JA, Im JS, et al. Senescence-associated β-galactosidase is lysosomal β-galactosidase. Aging Cell 2006;5:187–195.
92. Ezawa I, Sawai Y, Kawase T, et al. Novel p53 target gene FUCA1 encodes a fucosidase and regulates growth and survival of cancer cells. Cancer Sci 2016;107:734–745.
93. Hildebrand DG, Lehle S, Borst A, et al. α-Fucosidase as a novel convenient biomarker for cellular senescence. Cell Cycle 2013;12:1922–1927.
94. García-prat L, Martínez-Vicente M, Perdiguero E, et al. Autophagy maintains stemness by preventing senescence. Nature 2016;529:37–42.
95. Gerencser AA, Mookerjee SA, Jastroch M, et al. Positive feedback amplifies the response of mitochondrial membrane potential to glucose concentration in clonal pancreatic beta cells. Biochim Biophys Acta Mol Basis Dis 2017;1863:1054–1065.
96. Miwa S, Brand MD. Mitochondrial matrix reactive oxygen species production is very sensitive to mild uncoupling. Biochem Soc Trans 2003;31:1300–1301.
97. Turrens JF. Mitochondrial formation of reactive oxygen species. J Physiol 2003;552:335–344.
98. Nicholls DG. Mitochondrial membrane potential and aging. Aging Cell 2004;3:35–40.
99. Hanna H, Mir LM, Andre FM. In vitro osteoblastic differentiation of mesenchymal stem cells generates cell layers with distinct properties. Stem Cell Res Ther 2018;9: 203.
100. Lee HJ, Choi BH, Min BH, et al. Changes in surface markers of human mesenchymal stem cells during the chondrogenic differentiation and dedifferentiation processes in vitro. Arthritis Rheum 2009;60:2325–2332.
101. Bakshi S, McKee C, Walker K, et al. Toxicity of JQ1 in neuronal derivatives of human umbilical cord mesenchymal stem cells. Oncotarget 2018;9:33853–33864.
102. Rowland AL, Xu JJ, Joswig AJ, et al. In vitro MSC function is related to clinical reaction in vivo. Stem Cell Res Ther 2018;9:295.
103. Swartzlander MD, Blakney AK, Amer LD, et al. Immunomodulation by mesenchymal stem cells combats the foreign body response to cell-laden synthetic hydrogels. Biomaterials 2015;41:79–88.
104. Chabannes D, Hill M, Merieau E, et al. A role for heme oxygenase-1 in the immunosuppressive effect of adult rat and human mesenchymal stem cells. Blood 2007;110: 3691–3695.
105. Li L, Du G, Wang D, et al. Overexpression of heme oxygenase-1 in mesenchymal stem cells augments their protection on retinal cells in vitro and attenuates retinal

ischemia/reperfusion injury in vivo against oxidative stress. Stem Cells Int 2017;2017:4985323.
106. Sempere JM, Martinez-Peinado P, Arribas MI, et al. Single cell-derived clones from human adipose stem cells present different immunomodulatory properties. Clin Exp Immunol 2014;176:255–265.
107. François M, Romieu-Mourez R, Li M, et al. Human MSC suppression correlates with cytokine induction of indoleamine 2,3-dioxygenase and bystander M2 macrophage differentiation. Mol Ther 2012;20:187–195.
108. Liu Y, Zou X, Chai Y, et al. Macrophage polarization in inflammatory diseases. Int J Biol Sci 2014;10:520–529.
109. Mandal P, Pratt BT, Barnes M, et al. Molecular mechanism for adiponectin-dependent m2 macrophage polarization link between the metabolic and innate immune activity of full-length adiponectin. J Biol Chem 2011;286: 13460–13469.
110. Ndisang JF, Mishra M. The heme oxygenase system selectively suppresses the proinflammatory macrophage M1 phenotype and potentiates insulin signaling in spontaneously hypertensive rats. Am J Hypertens 2013;26:1123–1131.
111. Jadhav A, Tiwari S, Lee P, et al. The heme oxygenase system selectively enhances the anti-inflammatory macrophage-m2 phenotype, reduces pericardial adiposity, and ameliorated cardiac injury in diabetic cardiomyopathy in zucker diabetic fatty rats. J Pharmacol Exp Ther 2013;345:239–249.
112. Higashimura Y, Naito Y, Takagi T, et al. Preventive effect of agaro-oligosaccharides on non-steroidal anti-inflammatory drug-induced small intestinal injury in mice. J Gastroenterol Hepatol 2014;29:310–317.
113. Chen X, Wu S, Tang L, et al. Mesenchymal stem cells overexpressing heme oxygenase-1 ameliorate lipopolysaccharide-induced acute lung injury in rats. J Cell Physiol 2019;234: 7301–7319.

Address correspondence to:
Josh Erndt-Marino, PhD
Department of Biomedical Engineering
Tufts University
419 Boston Ave
Medford, MA 02155

E-mail: josh.marino2@gmail.com

Mariah S. Hahn, PhD
Department of Biomedical Engineering
Rensselaer Polytechnic Institute
110 8th Street
Troy, NY 12180-3522

E-mail: hahnm@rpi.edu